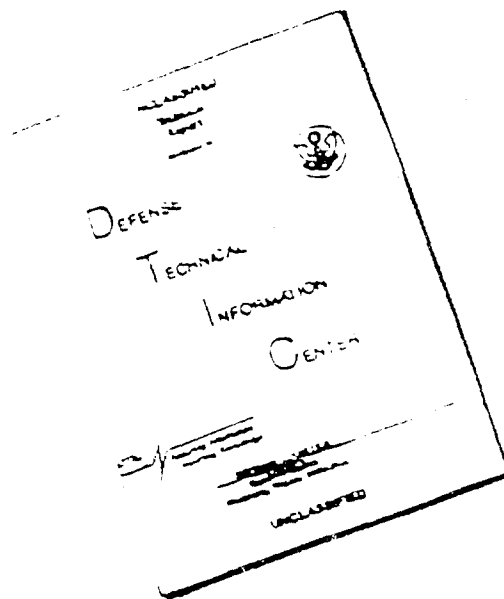# UNCLASSIFIED

AD 291 648

Reproduced
by the

ARMED SERVICES TECHNICAL INFORMATION AGENCY
ARLINGTON HALL STATION
ARLINGTON 12, VIRGINIA

UNCLASSIFIED

DISCLAIMER NOTICE

THIS DOCUMENT IS BEST QUALITY AVAILABLE. THE COPY FURNISHED TO DTIC CONTAINED A SIGNIFICANT NUMBER OF PAGES WHICH DO NOT REPRODUCE LEGIBLY.

Metals Research Laboratory
Carnegie Institute of Technology
Pittsburgh 13, Pennsylvania

NUCLEATION RATES IN THE ALPHA TO BETA TRANSFORMATION OF TIN

by

C. G. Durdaller, W. H. Robinson and G. M. Pound

Technical Report to the Office of Naval Research

Contract Nonr 760(08)

NUCLEATION RATES IN THE ALPHA TO BETA TRANSFORMATION OF TIN[*]

C. G. Durdaller, University of Pennsylvania, W. H. Robinson
and
G. M. Pound[**], Carnegie Institute of Technology

Abstract

The nucleation rate of the alpha (gray) to beta (white) tin transformation was measured as a function of temperature and alpha tin particle size by an x-ray diffraction technique. The powder specimens of alpha tin were essentially monodisperse and the small dimension of the particles of these specimens was varied from 13 to 75 microns. The fraction isothermally transformed as a function of time was determined continually from integrated intensity measurements of the 220 x-ray reflection of alpha tin. Inasmuch as the period for propagation of the beta phase is negligible in such small particles and since there was not internucleation between particles, it was possible to obtain the nucleation rate directly from the transformation data.

Several types of nucleation sites of differing potency were found to be operative in the nucleation process. It could not be determined whether these sites were on the free surface of the tin particles or within the volume. Assuming that they were on the free surface, the average density of the most potent sites was calculated to be 2.5 to 5.3 x 10^3 sites/cm^2 through the application of a Poisson distribution function to the isothermal data. Analysis of the temperature dependence of the rate constants at a given fraction transformed suggests that the active sites are regions of higher free energy and not catalytic interfaces. Appreciable induction periods were observed at the lower temperatures of transformation. They may be described in terms of a theory relating to the effect of decreased atomic mobility in delaying the establishment of a steady-state distribution of embryos.

Introduction

Experimental studies[1] of solid-solid phase transformations have led to the belief that the new phase nucleates at structural imperfections. The purpose of the present work was to learn more about the mechanism of nucleation in solids and the nature of the singularities at which nucleation occurs. In this investigation nucleation rates in the isothermal transformation of gray to white tin were measured by an x-ray diffraction technique using essentially monodisperse powders of gray tin. This particular phase transformation was chosen for study because it presented fewer experimental difficulties than most others. The experimental temperature-control problems were minimal because the two phases co-exist in equilibrium at 13.3°C, and measurable transformation rates occur at temperatures only slightly above room temperature. The growth rate of the beta phase into the alpha[2] is sufficiently fast to make the measured transformation rate equivalent to the nucleation rate, provided that the particle size of the samples is small enough; for the experimental temperatures used in this study, the particle diameter must be less than 100 microns.

Experimental Technique

The beta tin used in this study was obtained from Capper Pass and Son Ltd., North Ferriby, Yorkshire, England and was of 99.999% purity. It was transformed[3] to the alpha phase and ground into a fine powder in an agate mortar. This powder was separated by a Roller air classifier into seven fractions whose dimensions, as determined by microscopic measurement of many thousands of particles, are given in Table I and

TABLE I

True Means and Standard Deviation for the Particle Size Ranges

Range	Small Dimension (μ)	Large Dimension (μ)
1	13.14 ± 2.14	17.67 ± 3.16
2	20.10 ± 3.62	28.31 ± 5.25
3	27.11 ± 4.66	37.90 ± 6.66
4	31.22 ± 5.08	44.52 ± 8.19
5	41.31 ± 6.81	57.05 ± 8.90
6	53.33 ± 7.28	72.44 ± 12.06
7	69.64 ± 8.51	90.92 ± 12.40

whose distribution of size within each fraction is given in Figs. 1 and
2. The shape of the particles was roughly that of an oblate spheroid,
and the small dimension ranged from about 13μ to about 70μ for the
seven particle sizes. During all the powder-preparation steps the
powder was kept at a temperature well below the transformation temper-
ature; frequent checks were made using an x-ray diffractometer to
insure that no accidental transformation to the beta phase had occurred
during preparation.

An x-ray diffraction technique was used to measure the fraction
of alpha tin present at any time during the alpha to beta transformation.
The technique was similar to that used by Masson[4] in his study of the
effects of mechanical deformation on the bcc to hcp transformation in
β'AgCd. It differed only in that the integrated intensity of the alpha

diffraction line was measured, not the peak intensity. The relation,

$$\frac{I_\alpha}{I_{\alpha_p}} = W_\alpha \tag{1}$$

where I_α is the integrated x-ray intensity of the alpha diffraction line after the transformation has begun, I_{α_p} is the integrated intensity before the transformation has begun, and W_α is the weight fraction of alpha phase in the system, is valid only for a unary system.

A G.E. XRD-3 diffractometer equipped with an automatic counting circuit, which included a G.E. #5 SPG (Xenon filled) proportional counter, a Hamner N-302 amplifier and single channel pulse height analyzer, a ratemeter and recorder, and a Stabline voltage regulator and a line interference filter was used to supply an x-ray beam of constant intensity and to accurately record the intensity of the diffracted x-rays. The x-ray beam intensity was constant to $\pm 2\%$.

The specimen holder (Fig. 3) was mounted on the diffractometer. It contained a rotating sample mount (Fig. 4) to which the sample of alpha tin was bonded by means of rubber cement. The mixture of alpha tin and rubber cement was spread on the copper plate and, upon drying, was less than 0.01" in thickness. The sample was brought to temperature by pumping heated water into the specimen holder and directing it against the back of the thin copper plate on which the sample was mounted. A constant-temperature bath, which was controlled by a thermoregulator to $\pm 0.03°C$, supplied water to the specimen holder. The temperature of the bath was measured to $0.01 \pm 0.002_5°$ by a U.S. Bureau of Standards mercury-in-glass thermometer. Since the

calculated temperature drop across the plate upon which the sample was mounted (if all the heat loss of the apparatus is assumed to be concentrated in this plate) is only 0.004°C, the face of the plate was considered to be that of the bath. It was assumed that the sample was at the same temperature as the plate. In no case did the time for the face of the copper plate to reach temperature exceed four minutes.

The experimental procedure consisted of measuring the integrated intensity of the 220 reflection of alpha tin at 0°C before any transformation had begun. Then the transformation was initiated by starting the flow of water from the temperature bath and the integrated intensity of the diffraction line was measured continually until the transformation was stopped. A trace of the diffraction line was recorded (Fig. 5) and the background intensity determined by constructing the baseline for the reflection. Since the background intensity was not a function of the particular phase of tin present, it was considered to be constant throughout the transformation and thus was subtracted from each value of the total intensity recorded for the 220 reflection to give just the integrated intensity of the 220 reflection from the alpha phase fraction of the sample. The 220 reflection of alpha tin occurred at $2\theta = 17.80°$ (Mo K_α radiation) and the entire line could be scanned from $2\theta = 17.00$ to $19.00°$ in ten minutes. It was estimated that this x-ray method could determine the fraction of alpha phase present in the sample to $\pm 2\%$.

Experimental Results

1. The Nucleation Rate

The rate of nucleation of the alpha to beta tin transformation was determined as a function of particle size over a series of temperatures: 29.4, 31.8, 34.5, 36.5, 38.6 and 41.8°C. Typical experimental results for a single particle size over a range of temperatures are shown in Fig. 6, and for a single temperature over a range of particle sizes in Fig. 7.

From the experimental data of the fraction f of alpha phase transformed as a function of time, the first-order rate constant

$$k' = \frac{d \ln (f)}{dt} \tag{2}$$

was obtained by fitting the best smooth curve through the data and then taking the slopes of these curves at different fractions transformed. The rate constant decreased with decreasing temperature and particle size and also with increasing fraction transformed.

A series of experiments was conducted using one particle-size range at a temperature at which the samples were "pre-transformed" for varying periods of time. The results are shown in Fig. 8. The nucleation rate decreases with increasing times of pre-transformation, the decrease being greatest for the initial period of pre-transformation.

2. The Induction Period

In the measurement of the fraction isothermally transformed for all the particle-size ranges, a nucleation transient was observed. Further study of this transient, called the induction period, is

being undertaken and will be reported later. It suffices here to say
that these induction periods are outside the limits of experimental
error and can be most reasonably interpreted as the time required to
establish a steady-state distribution of alpha embryos after onset of
supersaturation. The induction period decreased with increasing
temperature and particle size; it increased with increasing time of
pre-transformation, the effect again being most pronounced during the
initial times of pre-transformation. Interpretation of these data
in terms of standard theory yielded an activation enthalpy ΔH_A for
the process of attaching an atom to the embryo of approximately
36 kcal/gram-atom.

Discussion

The experimental results given in Fig. 8 show that the nucleation
rate "constant" decreases with increasing fraction transformed. This
is strong evidence that the nucleation is heterogeneous. If it were
homogeneous the rate constant would not change with increase in
fraction transformed. Further the curves in Fig. 8 would all super-
impose. Thus the data imply that nucleation takes place at preferred
sites in the alpha tin, sites whose number progressively diminishes
as the transformation proceeds. Also it seems likely that there are
several types of sites present in these systems.

Accordingly the following analysis assumes that the nucleation
takes place at preferred sites, that each type of site is characterized
by a single rate constant and that the sites are independent of one
another and scattered throughout the system according to the Poisson

distribution function. An equation which was derived by Kimball[5] can be used to describe the nucleation process outlined above for particles of uniform size. This relationship is

$$P(\alpha) = \sum_j \exp \left\{ - m_j \left(1 - e^{-\bar{k}_j (t - \tau_j)} \right) \right\} \tag{3}$$

in which $P(\alpha)$ is the fraction of the particles (alpha phases) untransformed at time t, m_j is the arithmetic average number of nucleation sites of type j per particle, and $\bar{k}_j$ is the first-order rate constant for the jth site. It is understood that the terms on the right-hand side contribute to $P(\alpha)$ only when $t > \tau_j$.

Equation (3) can be solved readily[5] for a single site, but for several sites the solution becomes more complex requiring knowledge of the induction period τ_j for each site. Since this information is not at hand, equation (3) can be applied only to the portion of the data where but a single type of site is operative. In this case

$$P(\alpha) = \exp \left\{ m \left(1 - e^{-\bar{k} (t - \tau)} \right) \right\}. \tag{4}$$

If the picture of nucleation assumed here is correct, it should be possible to fit equation (4) to the initial portion of the data under the following conditions:

1) that m, the arithmetic average number of the most active sites per particle, is independent of the temperature of transformation and is a function only of particle size of the system, and

2) that $\bar{k}$, the first-order rate constant for the most active site, is independent of particle size.

Equation (4) was fitted to a single set of data (34.5°C, particle size #6) and thus $\bar{k}$ and m were obtained for this particular temperature and particle size. This value of $\bar{k}$ was then assumed to describe the rest of the data at this temperature, and the values of m for the other particle sizes were computed from equation (4). These values of m were used to solve for the rate constants at the different temperatures, and these rate constants, in turn, were used to check the values of m of the other particle sizes at each temperature.

Table II lists the values of the rate constants $\bar{k}$ for each temperature. Table III gives the values of m for the various particle sizes at each temperature. Figures 9 and 10 illustrate the nature of a typical fit of equation (4) to the experimental data. No attempt was made to fit equation (4) to the data taken at 41.3°C because of the high probability of a second type of nucleation site entering into the transformation process at early times (after less than 60 minutes). The fit of equation (4) to the initial portions of the experimental

TABLE II

The Kimball Rate Constants

T in °C	$\bar{k} \times 10^{-2}$ in min^{-1}
29.4	0.0253
31.8	0.0790
34.5	0.409
36.5	0.916
38.6	2.03

TABLE III

Values of m for the Particle Size Ranges

Particle Size Range	m (in sites per particle)				
	29.4°C	31.8°C	34.5°C	36.5°C	38.6°C
1	------	------	0.145	------	0.146
2	------	------	0.244	0.264	0.219
3	------	------	0.244	0.296	0.270
4	------	------	0.336	0.419	0.411
5	------	0.436	0.485	0.621	0.515
6	0.846	0.846	0.846	0.846	0.846
7	------	1.90	1.52	1.80	------

curves is very good for all the other data. Figures 9 and 10 show that the data are fitted for longer periods of time at the lower temperatures. The degree to which the two required conditions are fulfilled in fitting equation (4) to the data may be judged by the variation of m (Table III) for each particle size with temperature. This variation does not seem excessive when one considers that there is a distribution in size within each particle-size range and that there is some uncertainty in the value of m for particle size #6.

The variation of m with particle size should indicate where the nucleation sites are located. If the sites are located on the particle surface, m would be proportional to the surface area of the particle, while if the sites are located in the volume, m would be proportional to particle volume. An analysis of this type was carried out, but the

results were inconclusive. However, assuming that the active sites were on the surface, the density of these most active sites was calculated using m and the values of surface area, and this density is 2.5 to 5.3 x 10^3 sites/cm^2.

The nucleation rate may be written as[6]

$$J = Z \ s(i)^* \ \omega_i \ n \ \exp \ (-\Delta G_i^*/kT) \tag{5}$$

where Z is the Zeldovich factor which accounts for the departure of the steady-state from the equilibrium concentration of critical nuclei, $s(i)^*$ is the surface area of the critical nucleus, n is the concentration of single atoms, k is Boltzmann's constant, T is the absolute temperature and i is the number of atoms. The frequency of attachment of an atom to a unit area of critical nucleus in a condensed system is given by

$$\omega_i = \alpha \ (\frac{1}{d^2}) \ \nu \ \exp \ (\frac{\Delta S_A}{K}) \ \exp \ (-\frac{\Delta H_A}{kT}) \tag{6}$$

in which α is the probability of the atom moving in the proper direction, ν is the atomic vibrational frequency, ΔS_A and ΔH_A are the entropy and the enthalpy of activation for movement to the critical nucleus and d is the diameter of an atom. The free energy of formation of the critical nucleus in solid-solid nucleation may be written as

$$\Delta G_i^* = \frac{A \ \gamma'^3}{(\Delta G_V + \sigma + E)^2} \tag{7}$$

where A is a constant dependent on the shape of the critical nucleus, γ' is the specific interfacial free energy between the alpha nucleus

and the unstable beta phase, ΔG_v is the chemical free-energy difference per unit volume between the alpha and beta phases, σ is the difference in free energy per unit volume between the nucleation site and the beta phase (provided the site transforms) and E is the increase in strain energy per unit volume of nucleus formed.

The first-order rate constant per particle for a solid-solid nucleation process that takes place at preferred sites on the surface of particles of the unstable phase can be written as

$$k' = Z\, a_p\, f_A\, s(i)^*\, \omega_i\, n_s\, \exp\left(-\Delta G^*(i)/kT\right) \tag{8}$$

in which a_p is the surface area of a particle, f_A is the fraction of that area covered by preferred sites, and n_s is the concentration of atom sites on the surface. The Kimball rate constant for the site itself is

$$\bar{k} = k'/m\, . \tag{9}$$

Equations (8) and (9), when combined with equations (6) and (7), can be rewritten to express the temperature dependence of the rate constants:

$$\frac{k'\, \exp\left(-\Delta H_A/kT_1\right)}{\exp\left(-\Delta H_A/kT\right)} = B'\, \exp\left[\frac{-C}{k(\Delta G_v + \sigma + E)^2 T}\right] \tag{10}$$

where $B' = Z\, a_p\, f_A\, s(i)^*\, \alpha\, \left(\frac{1}{d^2}\right)\, \nu\, n_s\, \exp\left(\frac{\Delta S_A}{k}\right)\, \exp\left(-\frac{\Delta H_A}{kT_1}\right)$ and $C = A\gamma'^3$;

$$\frac{\bar{k}\, \exp\left(-\Delta H_A/kT_1\right)}{\exp\left(-\Delta H_A/kT\right)} = \bar{B}\, \exp\left[\frac{-C}{k(\Delta G_v + \sigma + E)^2 T}\right] \tag{11}$$

where $\overline{B} = B'/m$. The equations are put into this form to include most of the error in the value of ΔH_A in the constants B' and $\overline{B}$. The variation of B' and $\overline{B}$ with temperature would have a negligible effect on k' and $\overline{k}$ as compared with the experimental dependence on $1/T$. For this system, ΔG_V is given by $\Delta H_V (T_o-T)/T_o$ and $\Delta H_V = + 30.8$ cal/cm^3 and $T_o = 286.5^o$K. Figure 11 is a plot of k' exp $(-\Delta H_A/kT_1)$/exp $(-\Delta H_A/kT)$ versus $1/(\Delta G_V + \sigma + E)^2 T$ for $(\sigma + E) = -2000$ cal/gm atom and for 90% alpha tin present. Similar plots were prepared for $(\sigma + E) = 0$, -100 and -1000 cal/gm atom and for 90, 80 and 70% alpha tin present. No initial rate constants (100% alpha tin) were used because of the difficulty in measuring those constants; no data for the lower percentages of alpha tin or for 41.8°C were included because of the probability that more than one type of site contributed to the process. These plots illustrated the general characteristic that as $|\sigma + E|$ is increased a better linear fit of the data is obtained. Since E is always a positive contribution this evidence suggests, but certainly does not demonstrate, that σ is negative and may be of the order of several thousand calories per gram atom. This implies that the most active sites for nucleation in this transformation were regions of high energy on or in the gray tin particles.

Summary

An x-ray diffraction technique was used to measure solid-solid nucleation rates in the transformation of specimens of monodisperse alpha (gray) tin particles to the beta phase as a function of particle

size and temperature.

The nucleation rate constants were analyzed assuming that the nucleation sites were distributed among the particles according to the Poisson distribution function. This analysis permitted the calculation of the average number of sites per particle as well as the nucleation rate constant for the site. Assuming that the nucleation occurred on the surface of the gray tin particles, the density of the most potent sites was calculated to be 2.5 to 5.3 x 10^3 per cm^2.

The temperature dependence of the rate constants suggests that the catalytic sites were regions of high energy on or in the gray tin particles.

References

1. J. B. Newkirk, Acta Met. $\underline{4}$, 316 (1956).
    W. DeSorbo and D. Turnbull, Acta Met. $\underline{4}$, 495 (1956).
    R. E. Cech and D. Turnbull, Trans. AIME $\underline{212}$, 395 (1958).
    R. E. Cech and J. H. Hollomon, Trans. AIME $\underline{197}$, 685 (1953).

2. R. G. Wolfson, M. E. Fine and A. W. Ewald, J. Appl. Phys. $\underline{31}$, 1973 (1960).

3. E. S. Hedges and J. Y. Higgs, Nature $\underline{169}$, 621 (1952).

4. D. B. Masson, Acta Met. $\underline{8}$, 71 (1960).

5. G. M. Pound and V. K. LaMer, J. Amer. Chem. Soc. $\underline{74}$, 2323 (1952).

6. J. H. Hollomon and D. Turnbull, Progress in Metal Physics, Volume 4, Interscience Publishers, New York (1953), p. 333 ff.
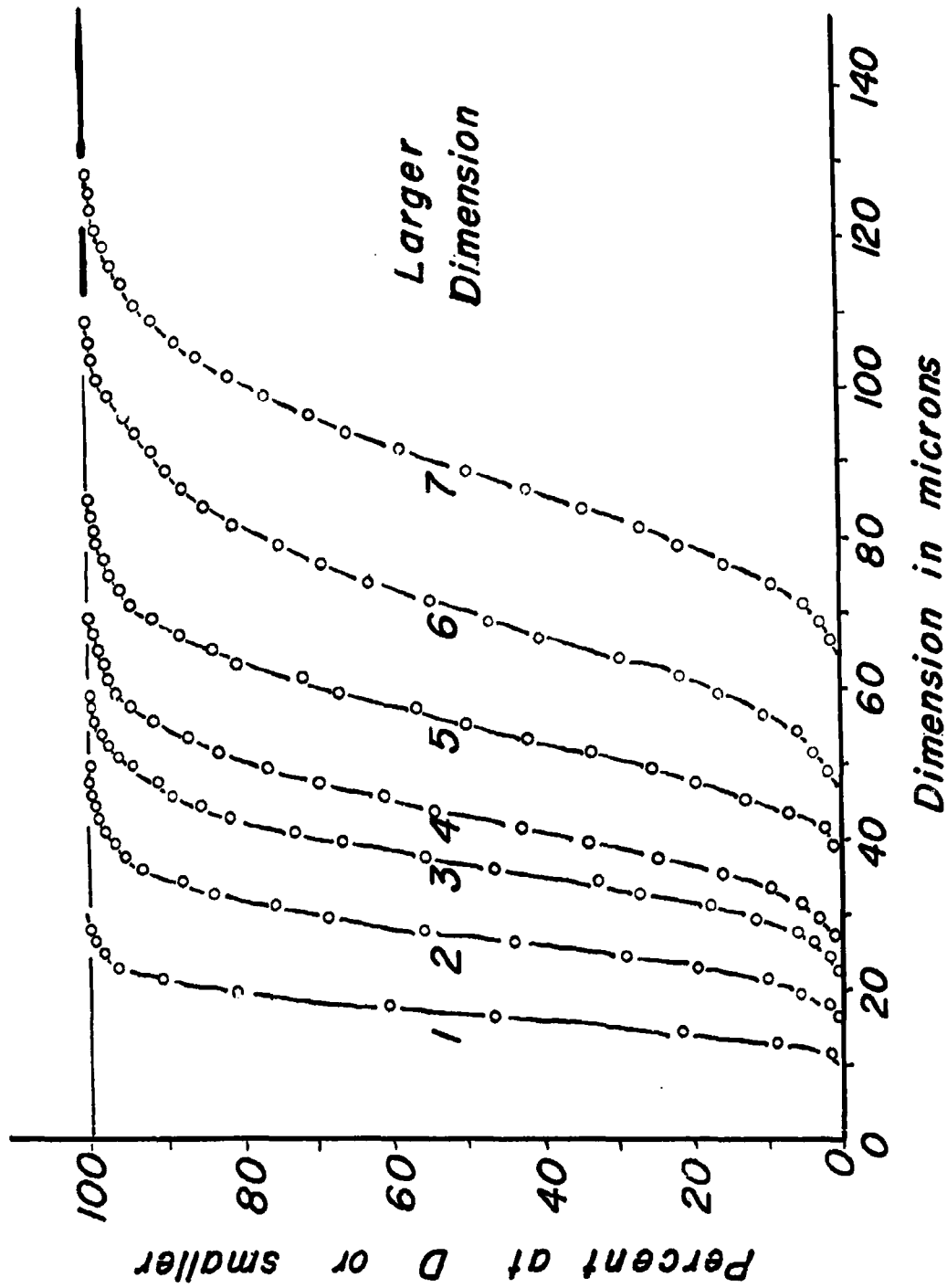
Figure Captions

Fig. 1. Ogive plot of the large dimension of alpha tin particles.

Fig. 2. Ogive plot of the small dimension of alpha tin particles.

Fig. 3. Side view of specimen holder for heating and pinning the specimen on diffractometer.

Fig. 4. Method of mounting sample on specimen holder.

Fig. 5. The alpha tin 220 diffraction line.

Fig. 6. Plot of the percent alpha tin versus time of transformation for constant particle size.

Fig. 7. Plot of the percent alpha tin versus time of transformation for constant temperature.

Fig. 8. Plot of the percent alpha tin versus time of transformation for various times of pre-transformation.

Fig. 9. Plot of the percent alpha tin versus time of transformation for constant particle size and the Kimball relation.

Fig. 10. Plot of the percent alpha tin versus time of transformation for constant temperature and the Kimball relation.

Fig. 11. Plot of $\log B' + \Delta H_A (T_1-T)/kTT_1$ and $\log \bar{k} + \Delta H_A (T_1-T)/kTT_1$ versus $1/(\Delta G_v + \sigma + E)^2 T$ for $(\sigma + E) = -2000$ cal/gm-atom.

Fig. 1. Ogive plot of the large dimension of alpha tin particles.

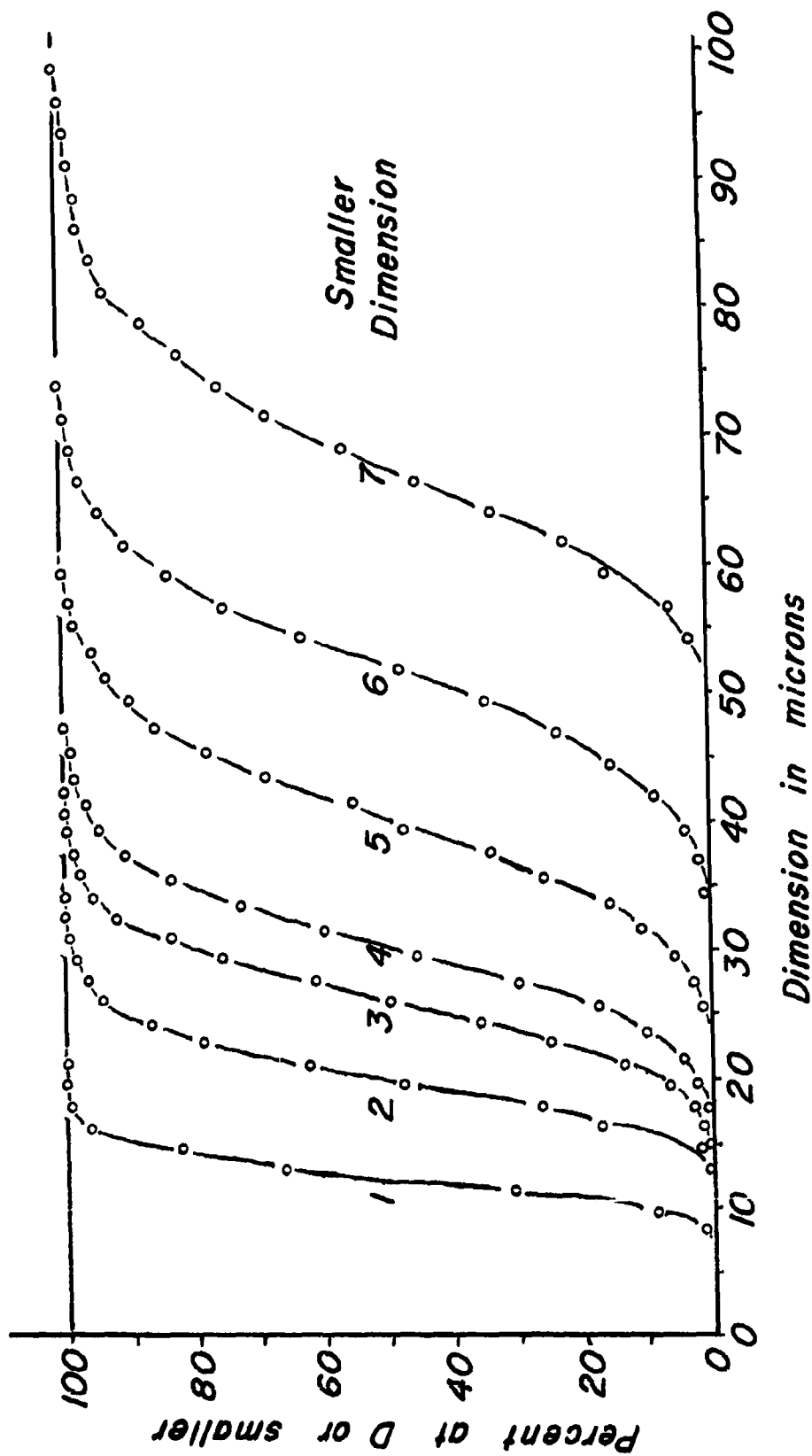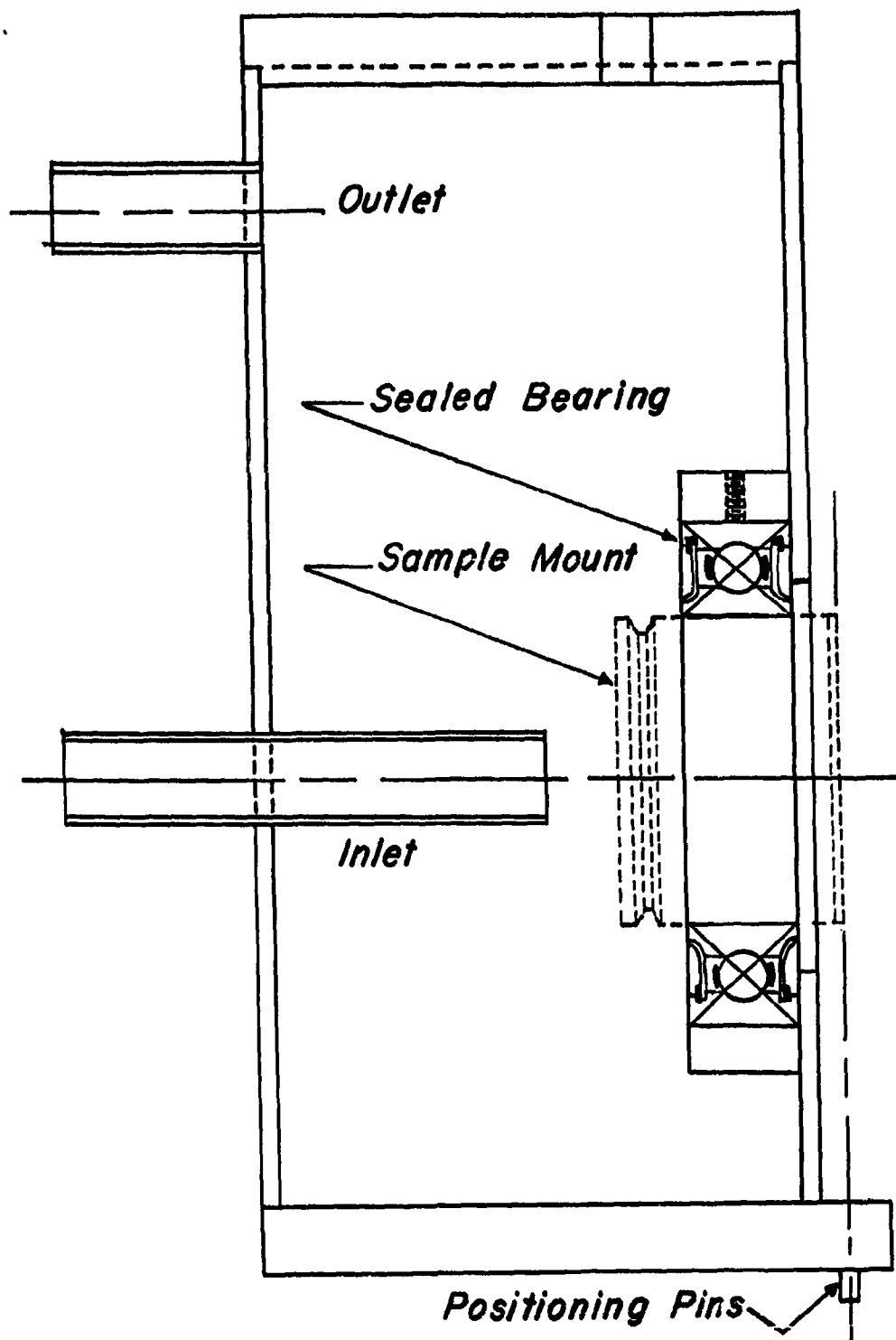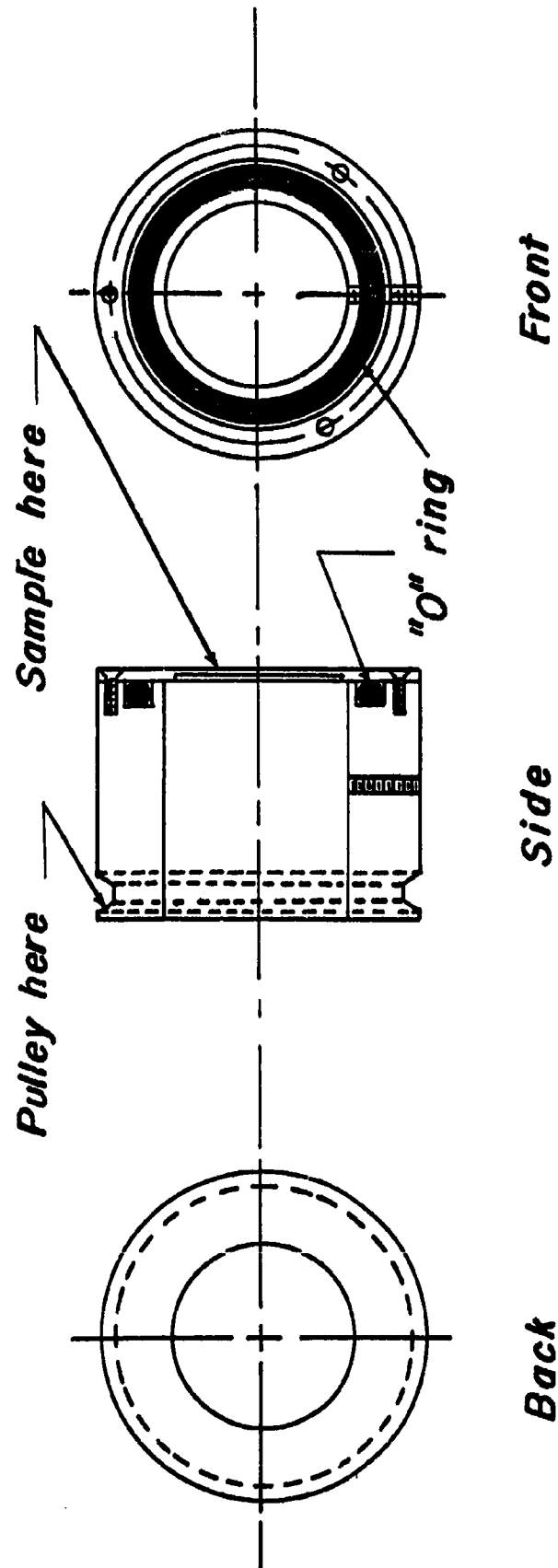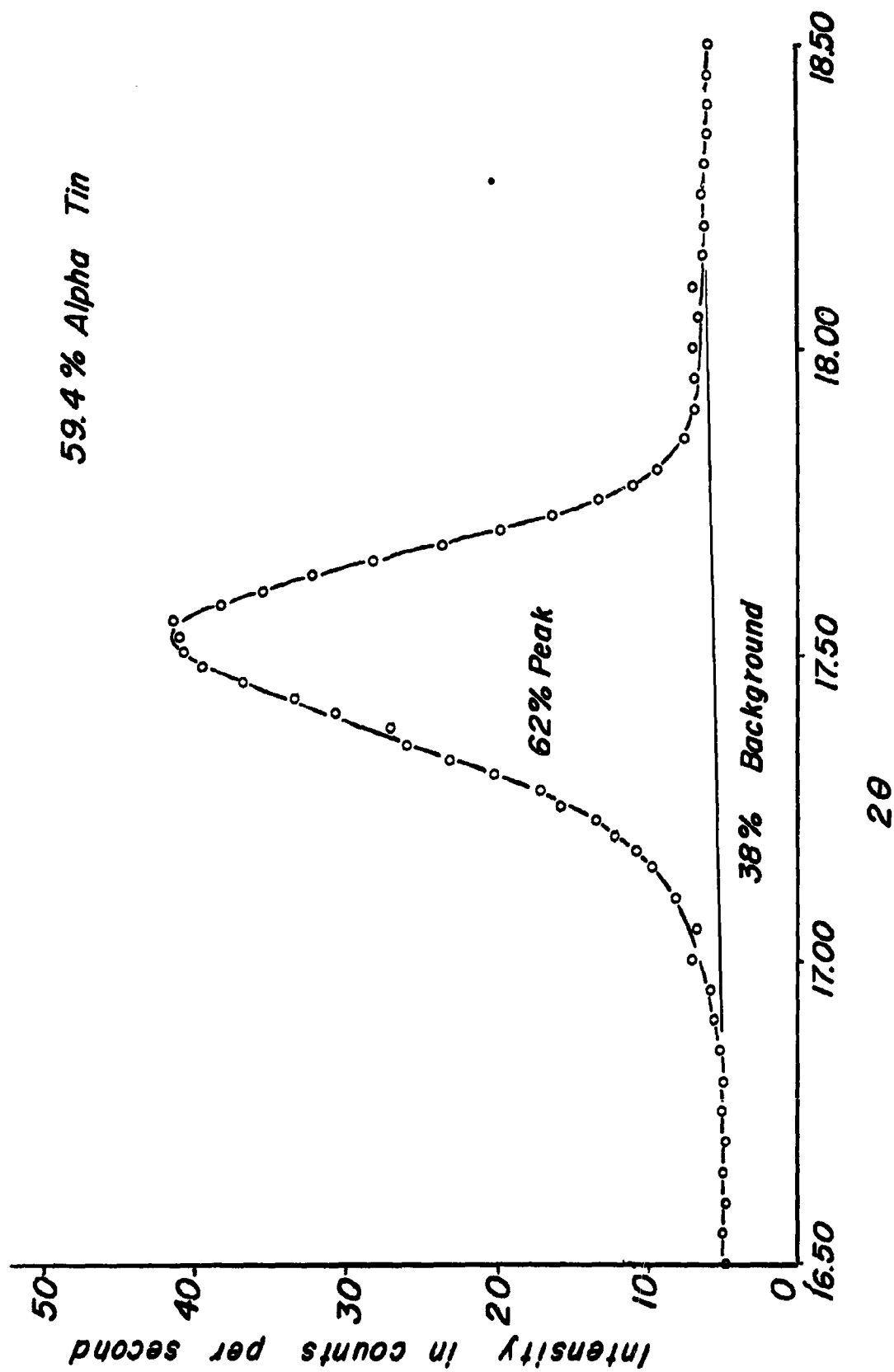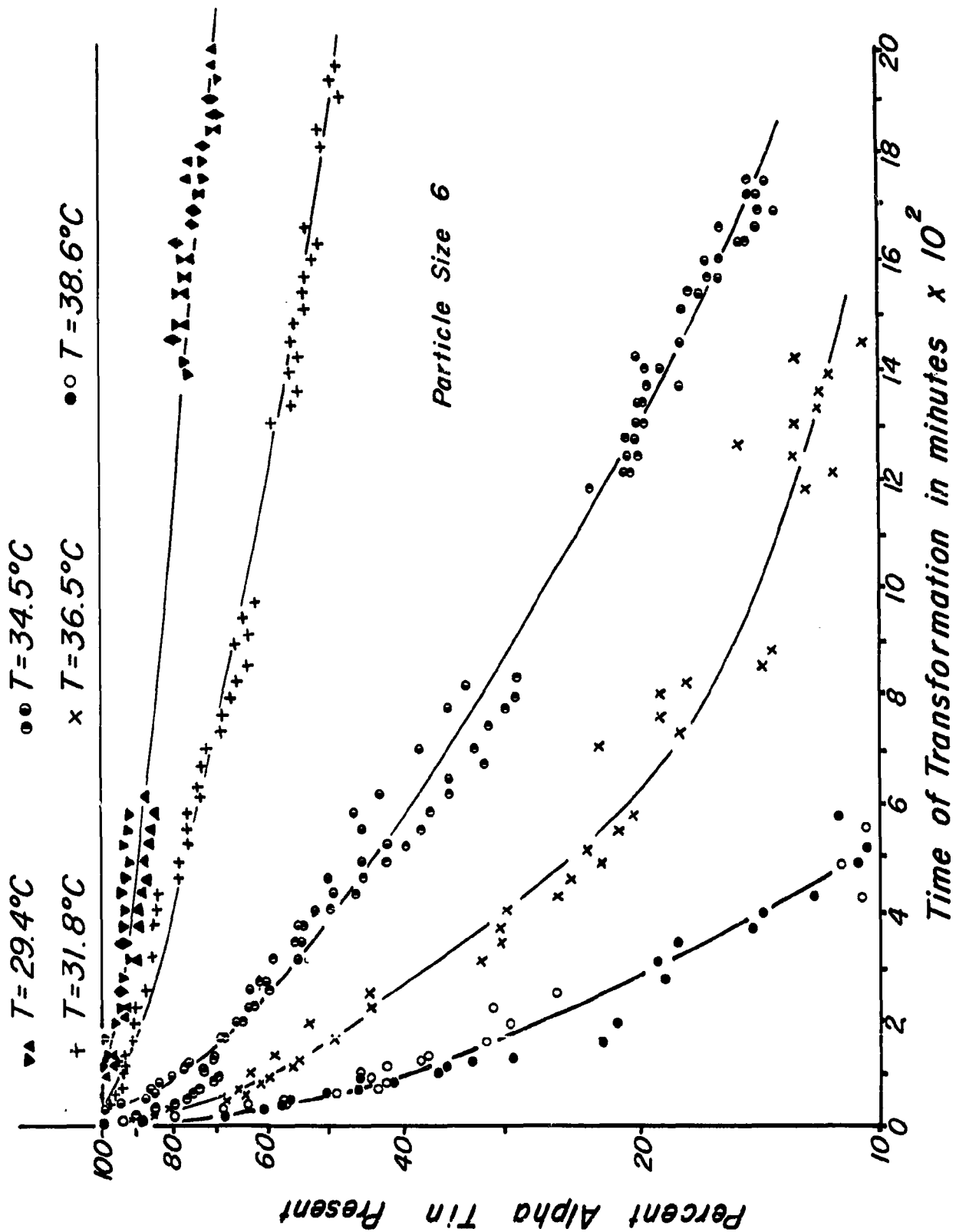Fig. 2. Ogive plot of the small dimension of alpha tin particles.

Outlet

Sealed Bearing

Sample Mount

Inlet

Positioning Pins

Sample Holder
Side View

Fig. 3. Side view of specimen holder for heating and pinning the
specimen on diffractometer.

Fig. 4. Method of mounting sample on specimen holder.

Fig. 5. The alpha tin 220 diffraction line.

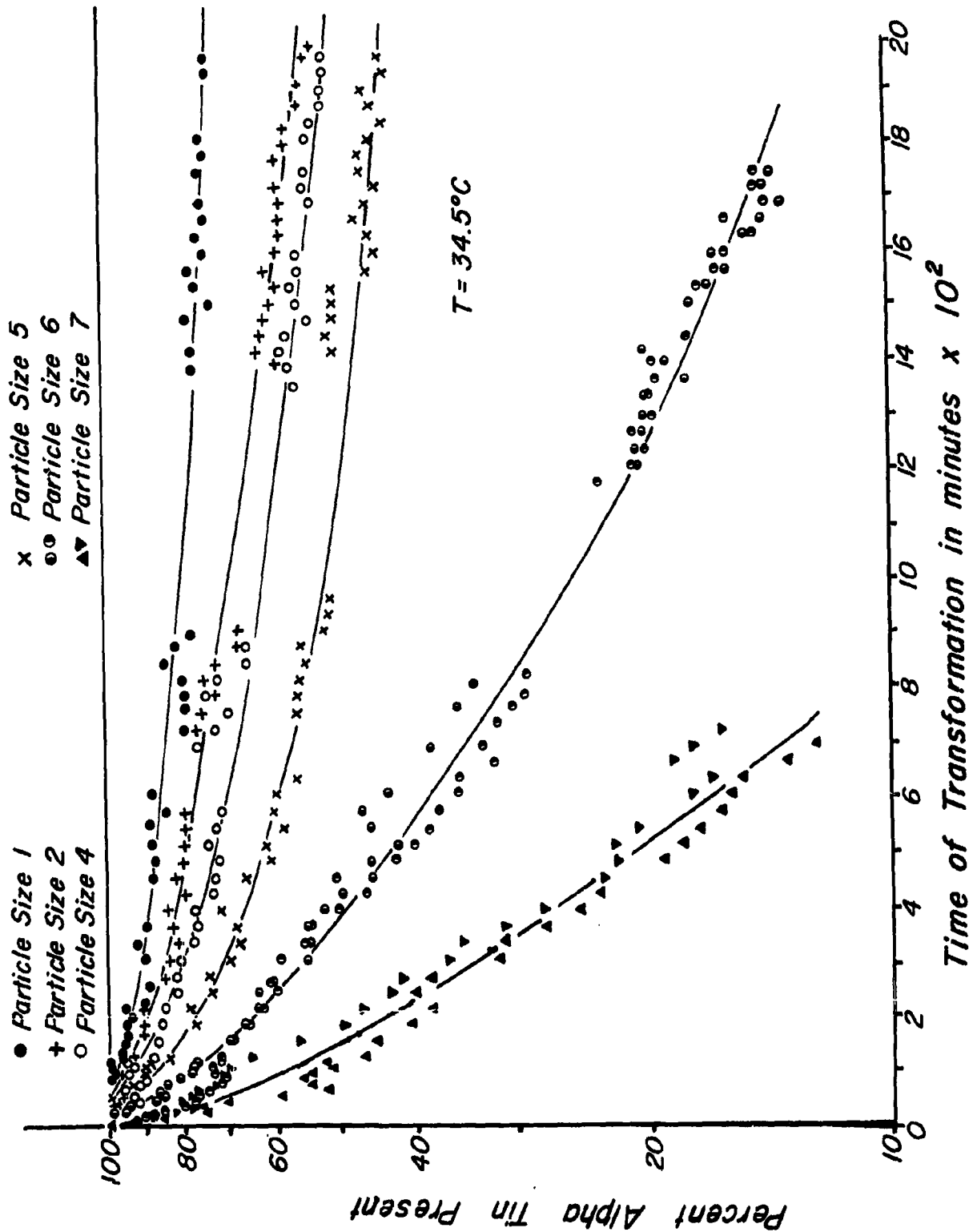Fig. 6. Plot of the percent alpha tin versus time of tranformation for constant particle size.

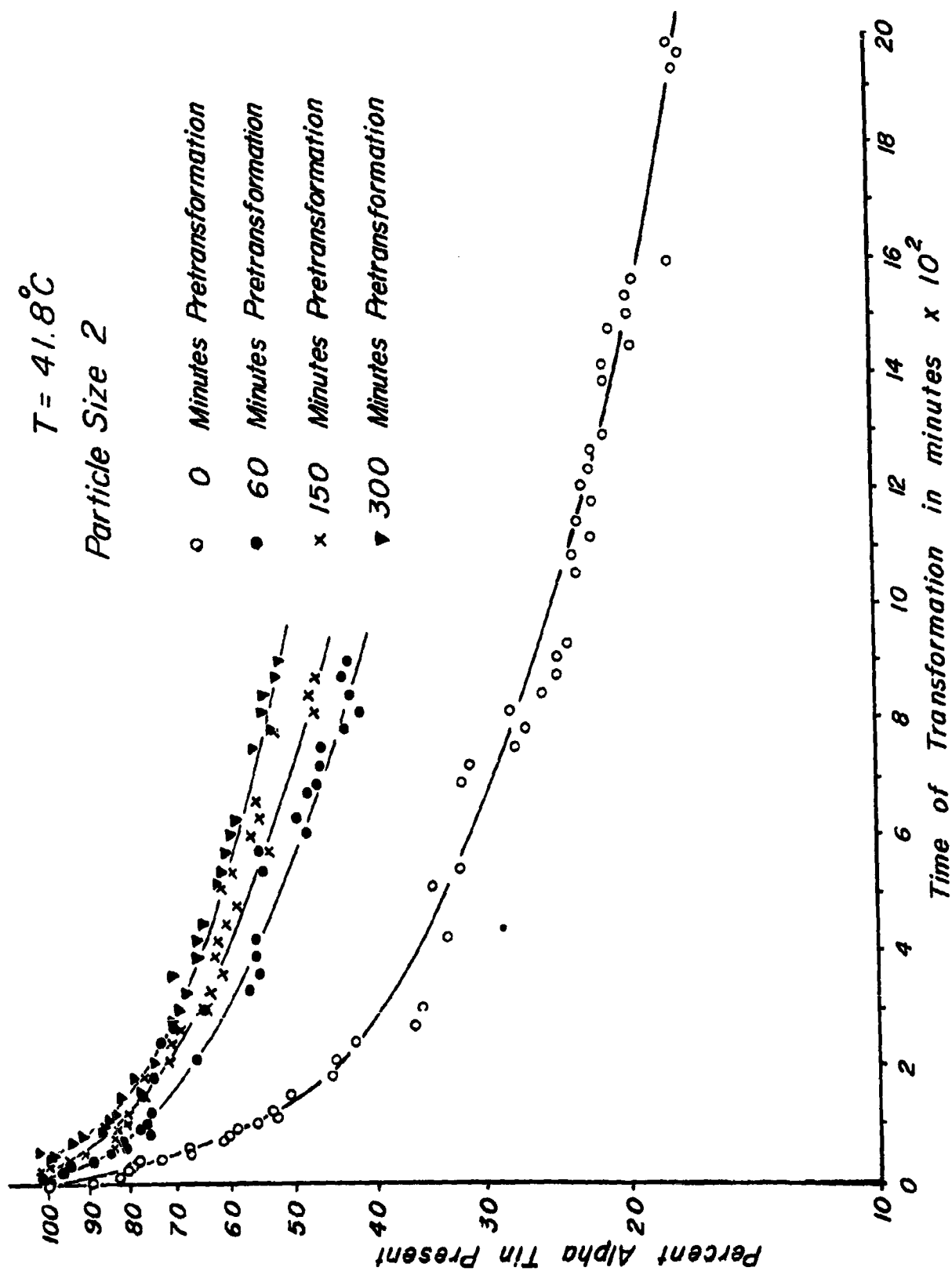Fig. 7. Plot of the percent alpha tin versus time of transformation for constant temperature.

Legend:
- • Particle Size 1
- + Particle Size 2
- ○ Particle Size 4
- × Particle Size 5
- ◐ Particle Size 6
- ▲▼ Particle Size 7

$T = 34.5°C$

Percent Alpha Tin Present

Time of Transformation in minutes $\times 10^2$

Fig. 8. Plot of the percent alpha tin versus time of transformation for various times of pre-transformation.
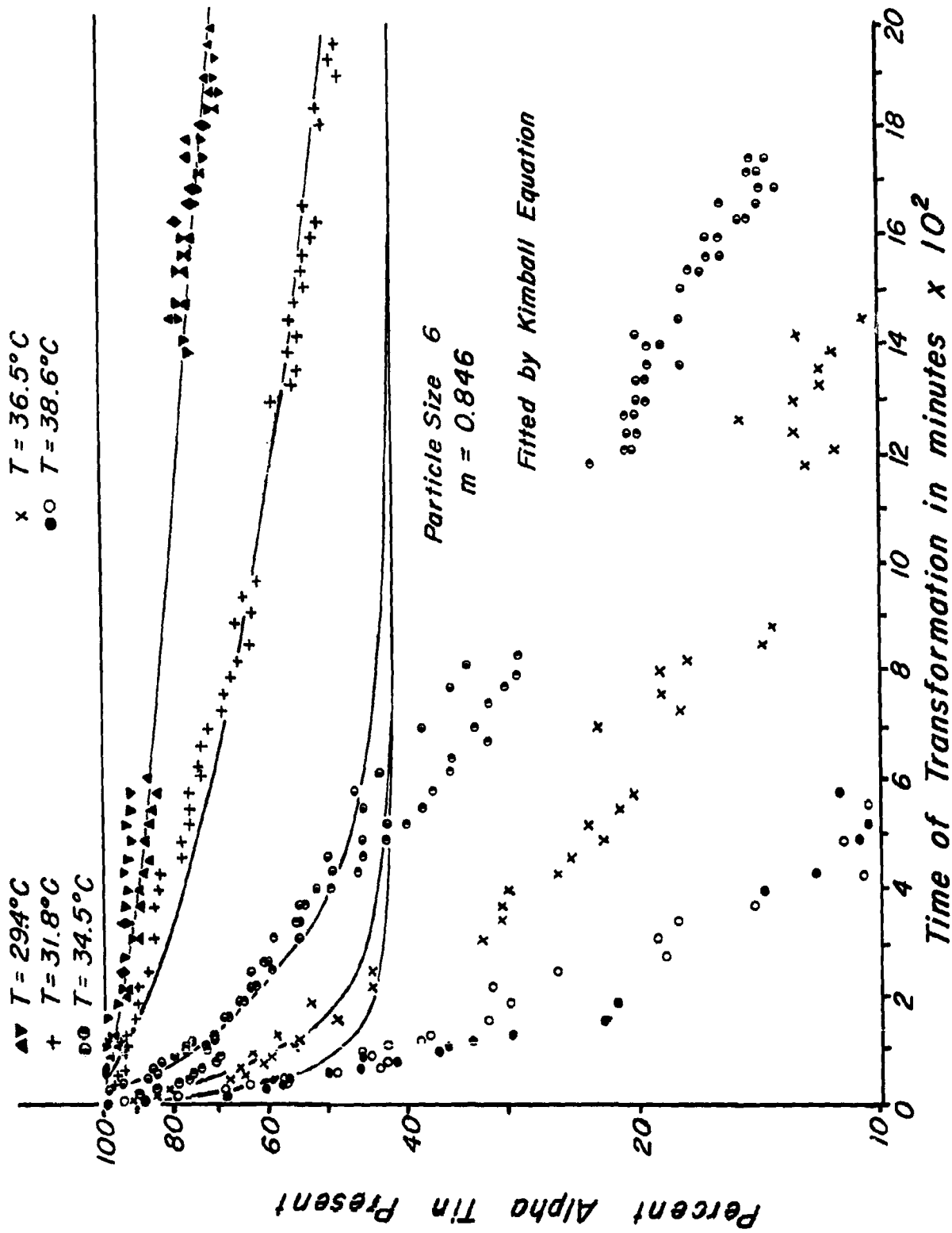
Fig. 9. Plot of the percent alpha tin versus time of transformation for constant particle size and the Kimball relation.
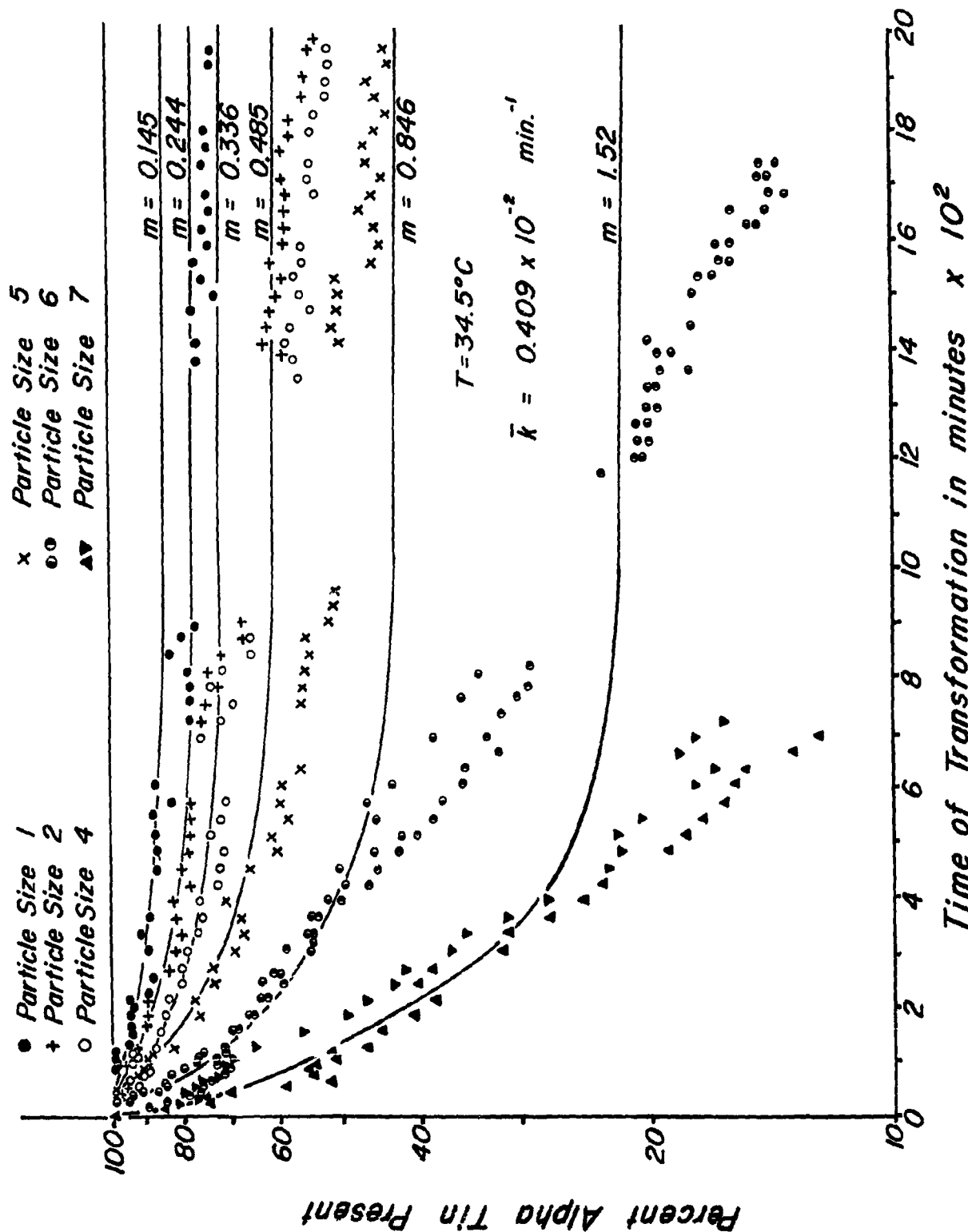
Fig. 10. Plot of the percent alpha tin versus time of transformation for constant temperature and the Kimball relation.
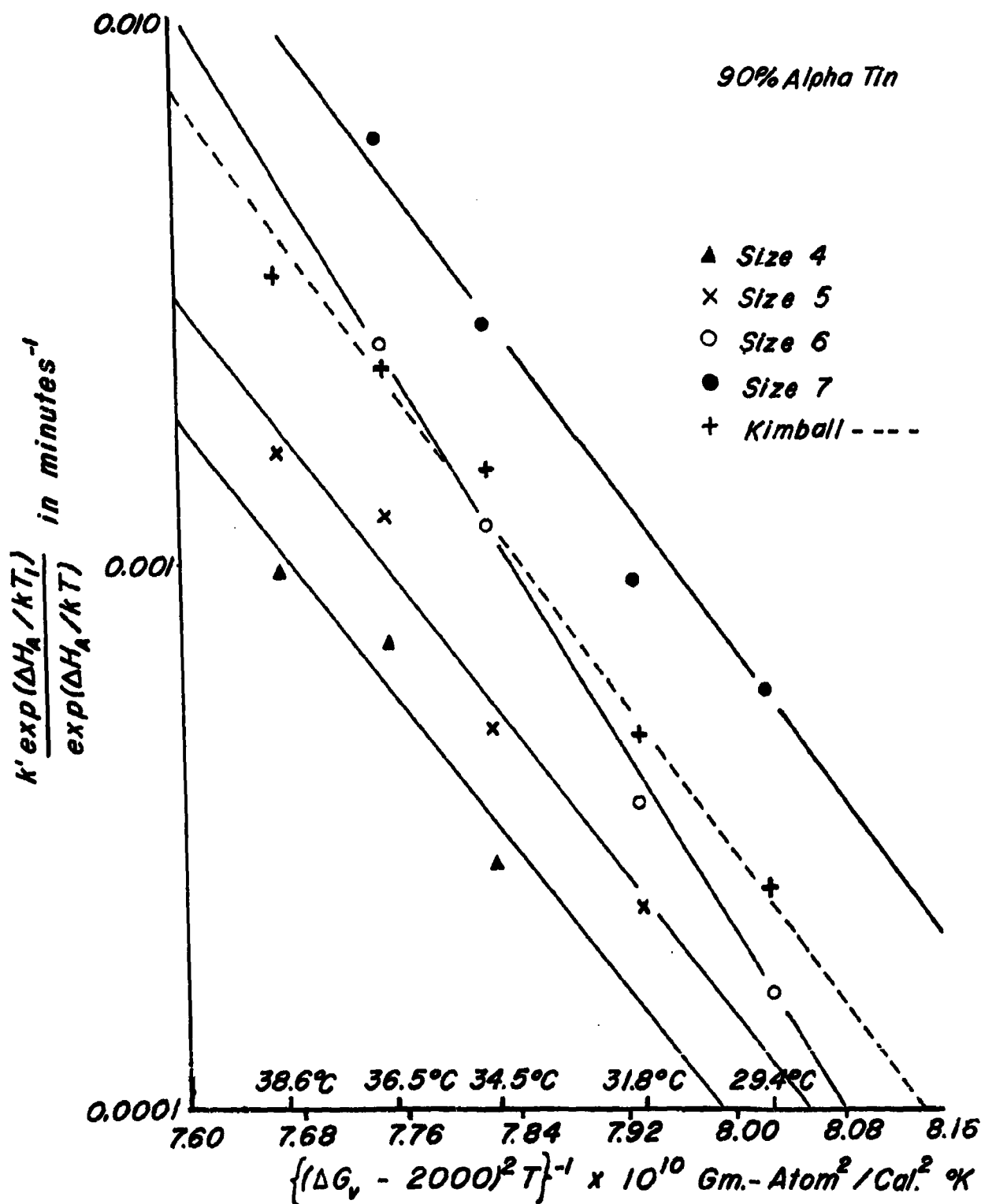
Fig. 11. Plot of $\log B' + \Delta H_A (T_1-T)/kTT_1$ and $\log \bar{k} + \Delta H_A (T_1-T)/kTT_1$ versus $1/(\Delta G_v + \sigma + E)^2 T$ for $(\sigma + E) = -2000$ cal/gm-atom.

UNCLASSIFIED

UNCLASSIFIED